Trypanosomal variant surface glycoprotein expression in human African trypanosomiasis patients

Jaime So[1]**, Sarah Sudlow[1]**, Abeer Sayeed[1], Tanner Grudda[1], Stijn Deborggraeve[2#], Dieudonné Mumba Ngoyi[3], Didier Kashiama Desamber[4], Bill Wickstead[5], Veerle Lejon[6], and Monica R. Mugnier[1]*

[1]Department of Molecular Microbiology and Immunology, Johns Hopkins Bloomberg School of Public Health, Baltimore, Maryland, United States of America

[2]Department of Biomedical Sciences, Institute of Tropical Medicine, Antwerp, Belgium

[3]Department of Parasitology, Institut National de Recherche Biomédicale, Kinshasa, Democratic Republic of the Congo

[4]Programme Nationale de Lutte contre la Trypanosomiase Humaine Africaine, (PNLTHA), Ministry of Health, Kinshasa, Democratic Republic of the Congo

[5] School of Life Sciences, Queen's Medical Centre, University of Nottingham, Nottingham, NG7 2UH, United Kingdom

[6] UMR-177 Intertryp, Institut de Recherche pour le Développement, Centre de Coopération Internationale en Recherche Agronomique pour le Développement, University of Montpellier, Montpellier, France

**These authors contributed equally to the work

Current address: Médecins Sans Frontières - Access Campaign, Geneva, Switzerland

* Corresponding author

E-mail: mmugnie1@jhu.edu (MM)

Abstract

Trypanosoma brucei gambiense, an extracellular protozoan parasite, is the primary causative agent of human African Trypanosomiasis. *T. b. gambiense* is endemic to West and Central Africa where it is transmitted by the bite of infected tsetse flies. In the bloodstream of an infected host, the parasite evades antibody recognition by altering the Variant Surface Glycoprotein (VSG) that forms a dense coat on its cell surface through a process known as antigenic variation. Each VSG has a variable N-terminal domain that is exposed to the host and a less variable C-terminal domain that is at least partially hidden from host antibodies. Our lab developed VSG-seq, a targeted RNA-seq method, to study *VSG* expression in *T. brucei*. Studies using VSG-seq to characterize antigenic variation in a mouse model have revealed marked diversity in *VSG* expression within parasite populations, but this finding has not yet been validated in a natural human infection. Here, we used VSG-seq to analyze *VSGs* expressed in the blood of twelve patients infected with *T. b. gambiense*. The number of *VSGs* identified per patient ranged from one to fourteen and, notably, two *VSGs* were shared by more than one patient. Analysis of expressed *VSG* N-terminal domain types revealed that 82% of expressed *VSGs* encoded a type B N-terminus, a bias not seen in datasets from other *T. brucei* subspecies. C-terminal types in *T. b. gambiense* infection were also restricted. These results demonstrate a bias either in the underlying *VSG* repertoire of *T. b. gambiense* or in the selection of *VSGs* from the repertoire during infection. This work demonstrates the feasibility of using VSG-seq to study antigenic variation in human infections and highlights the importance of understanding *VSG* repertoires in the field.

Author Summary

Human African Trypanosomiasis is a neglected tropical disease largely caused by the extracellular parasite known as *Trypanosoma brucei gambiense*. To avoid elimination by the host, these parasites repeatedly replace their dense surface coat of Variant Surface Glycoprotein (VSG). Despite the important role of VSGs in prolonging infection, *VSG* expression during natural human infections is poorly understood. A better understanding of natural *VSG* expression dynamics can clarify the mechanisms which *T. brucei* uses to alter its VSG coat and improve how trypanosomiasis is diagnosed in humans. We analyzed the expressed *VSGs* detected in the blood of patients with trypanosomiasis. Our findings indicate that a diverse range of *VSGs* are expressed in both natural and experimental infections.

Introduction

Human African Trypanosomiasis (HAT) is caused by the protozoan parasite *Trypanosoma brucei*. *T. brucei* and its vector, the tsetse fly, are endemic to sub-Saharan Africa [1]. There are two human-infective *T. brucei* subspecies: *T. b. gambiense* which causes chronic infection in West and Central Africa (~98% of cases) and *T. b. rhodesiense* which causes acute infection in East and Southern Africa (~2% of cases) [2,3]. In humans, infections progress from an early stage that is generally marked by a fever and body aches to a late stage that begins once the parasite crosses the blood-brain barrier and is accompanied by the development of severe neurological symptoms [4]. HAT is considered fatal without timely diagnosis and treatment. While around 50 million people are at risk of infection [5], the number of annual human infections has declined significantly in recent years, with only 864 cases reported in 2019 [6]. The World Health Organization is working towards zero human transmissions of HAT caused by *T. b. gambiense* (gHAT) by 2030 [7]. Current public health initiatives to control the disease depend on case detection and treatment, complemented with vector control.

Prospects for developing a vaccine are severely confounded by the ability of African trypanosomes to alter their surface antigens [8]. As *T. brucei* persists extracellularly in the blood, lymph, and tissue fluids of the host, it is constantly exposed to host antibodies[9–12]. To evade immune recognition, the parasite periodically changes its dense Variant Surface Glycoprotein (VSG) coat. This process, referred to as antigenic variation, relies on a vast collection of thousands of VSG-encoding genes[13–16]. *T. brucei* also continually expands the number of usable antigens by constructing mosaic *VSGs*—the result of one or more recombination events between individual *VSG* genes [17,18]

The VSG contains two domains: a variable N-terminal domain of ~350-400 amino acids and a less variable C-terminal domain of ~40-80 amino acids, characterized by one or two conserved groups of four disulfide-bonded cysteines [13,19]. On the surface of trypanosomes, the VSG N-terminal domain is readily exposed to the host, while the C-terminal domain is proximal to the plasma membrane and largely hidden from host antibodies [20–22]. The N-terminal domain has been classified into two types, A and B, each of which is classified into subtypes (A1-3 and B1-2). The C-terminal domain has been classified into six types (1-6) [13,19]. These classifications are based on protein sequence patterns anchored by the conservation of cysteine residues. The biological implications of these VSG domain types have not been investigated.

Little is known about how the large genomic repertoire of *VSGs* is used in natural infections; the number and diversity of *VSGs* expressed by wild parasite populations remains unknown. One VSG in particular, LiTat 1.3, has been identified as an antigen against which a large percentage of gHAT patients have antibodies [23]. As a result, LiTat 1.3 is the main target antigen in the primary serological screening tool used for gHAT, a test known as the card agglutination test for trypanosomiasis (CATT/*T.b. gambiense*)[24]. Despite the widespread use of the CATT to screen for gHAT there are

shortcomings: not only can the CATT provide false negatives, but there are also *T. b. gambiense* strains that lack the LiTat 1.3 gene entirely [25,26]. More recently developed rapid diagnostic tests use a combination of native LiTat1.3 and another VSG, LiTat1.5 [27,28], or a combination of a VSG with the invariant surface glycoprotein ISG 65 [29]. Currently there is no serological test for diagnosis of infection with *T. b. rhodesiense.*

Given the role of VSGs during infection and their importance in gHAT screening tests, a better understanding of *VSG* expression dynamics could inform the development of improved screening tests while providing insight into the molecular mechanisms of antigenic variation. We developed VSG-seq, a targeted RNA-sequencing method that identifies the *VSGs* expressed in any population of *T. brucei* and measures the prevalence of each VSG in the population [30]. In a proof-of-principle study, we used VSG-seq to gain insight into the number and diversity of *VSGs* expressed during experimental mouse infections [30]. This study revealed significant *VSG* diversity within parasite populations, yet found many of the same *VSGs* were expressed in different infections, supporting previous reports of a “semi-predictable” order to *VSG* switching [17,31,32]. Recently, similar high-throughput sequencing methods have been used to characterize antigenic variation in experimental infections of natural hosts for two related African trypanosome species, *T. vivax* and *T. congolense* [33–35], suggesting that the mechanism for antigen production in some animal parasites is different from the *T. brucei* model.

Whether or not findings from experimental studies of antigenic variation translate to natural *T. brucei* infections is currently unknown. To our knowledge, only one study has investigated *VSG* expression in wild *T. brucei* isolates [36]. For technical reasons, this study relied on RNA isolated from parasites that were passaged through small animals after collection from the natural host. As *VSG* expression may change during passage, the data obtained from these samples is somewhat difficult to interpret. To gain a better understanding of the characteristics of antigenic variation in natural *T. brucei* infections, we sought to analyze *VSG* expression in *T. brucei* field isolates from which RNA was directly extracted.

In this study, we used VSG-seq to determine the number and diversity of *VSGs* expressed by *T. b. gambiense* in the blood of twelve patients with a *T. b. gambiense* infection. To complement these data, we also analyzed published datasets from both experimental mouse infections and *T. b. rhodesiense* patients. Our analysis revealed that there is diverse expression of *VSGs* in natural *T. brucei* infections, and *T. b. gambiense* infections show distinct biases in *VSG* expression that may be unique to this subspecies.

Methods

Ethics statement

The blood specimens from *T.b. gambiense* infected patients were collected within the projects "Longitudinal follow-up of CATT seropositive, trypanosome negative individuals (SeroSui) and "An integrated approach for identification of genetic determinants for susceptibility for trypanosomiasis (TrypanoGEN) [37]. In France, the SeroSui study received approval from the "Comité Consultatif de Déontologie et d'Ethique" (CCDE) of the French National Institute for Sustainable Development Research (IRD, May 2013 session), and in Belgium from the Institutional Review Board of the Institute of Tropical Medicine (reference 886/13) and from the Ethics Committee of the University of Antwerp (B300201318039). In DR Congo, the projects SeroSui and TrypanoGEN were approved by the Ministry of Health through the Ngaliema Clinic of Kinshasa (references 422/2013 and 424/2013). Participants gave their written informed consent to participate in the projects. For minors, additional written consent was obtained from their legal representative.

Patient Enrollment and Origin Map

Patients originated from the Democratic Republic (DR) of the Congo and were identified in the second half of 2013, either during passive screening at the center for HAT diagnosis and treatment of the hospital of Masi Manimba, or during active screening by the mobile team of the national sleeping sickness control program (PNLTHA) in Masi Manimba and Mosango health zones (Kwilu province, DR Congo). Individuals were screened for the presence of specific antibodies in whole blood with the CATT test. For those reacting blood positive in CATT, twofold serial plasma dilutions of 1/2-1/32 were also tested and the CATT end titer was determined. CATT positives underwent parasitological confirmation by direct microscopic examination of lymph (if enlarged lymph nodes were present), and examination of blood by the mini-anion exchange centrifugation technique on buffy coat [38]. Individuals in whom trypanosomes were observed underwent lumbar puncture. The cerebrospinal fluid was examined for white blood cell count and presence of trypanosomes to determine the disease stage and select the appropriate treatment. The patients were questioned about their place of residence, the geographic coordinates of the corresponding villages were obtained from the atlas of HAT [39] and plotted on a map of the DR Congo using ArcGIS® software by Esri. Distances were determined and a distance matrix generated (see Supplemental Table 2).

Patient Blood Sample Collection and Total RNA Isolation

A 2.5 mL volume of blood was collected from each patient in a PAXgene Blood RNA Tube. The blood was mixed with the buffer in the tube, aliquoted in 2 mL volumes and frozen in liquid nitrogen for a maximum of two weeks. After arrival in Kinshasha, tubes were stored at -70°C. Total RNA was extracted and isolated from each blood sample as previously described [40].

Estimation of Parasitemia

Two approaches were used to estimate parasitemia. First, a 9 mL volume of blood on heparin was centrifuged, 500 microliters of the buffy coat were taken up and trypanosomes were isolated using the mini-anion exchange centrifugation technique. After centrifugation of the column eluate, the number of parasites visible in the tip of the collection tube were estimated. Second, Spliced Leader (SL) RNA expression levels were measured by real-time PCR as previously described [40]. A Ct value was determined for each patient blood sample. Real-time PCR was performed on RNA samples before reverse transcription to verify the absence of DNA contamination.

RNA-sequencing

DNase I-treated RNA samples were cleaned up with 1.8x Mag-Bind TotalPure NGS Beads (Omega Bio-Tek, # M1378-01). cDNA was generated using the SuperScript III First-strand synthesis system (Invitrogen, 18080051) according to manufacturer's instructions. Eight microliters of each sample (between 36 and 944 ng) were used for cDNA synthesis, which was performed using the oligo-dT primer provided with the kit. This material was cleaned up with 1.8x Mag-Bind beads and used to generate three replicate library preparations for each sample. These technical replicates were generated to ensure that any *VSGs* detected were not the result of PCR artifacts[41,42]. Because the number of parasites in each sample was expected to be low, we used a nested PCR approach for preparing these VSG-seq libraries. First, we amplified *T. brucei* cDNA from the parasite/host cDNA pool by PCR using a spliced leader primer paired with an anchored oligo-dT primer (SL-1-nested and anchored oligo-dT; Supplemental Table 1). 20 cycles of PCR were completed (55ºC annealing, 45s extension) using Phusion polymerase (Thermo Scientific, #F530L). PCR reactions were cleaned up with 1.8x Mag-Bind beads. After amplifying *T. brucei* cDNA, a *VSG*-specific PCR reaction was carried out using M13RSL and 14-mer-SP6 primers (see primers; Supplemental Table 1). 30 cycles of PCR (42ºC annealing, 45s extension) were performed using Phusion polymerase. Amplified *VSG* cDNA was then cleaned up with 1X Mag-Bind beads and quantified using a Qubit dsDNA HS Assay (Invitrogen Q32854). Sequencing libraries were prepared from 1 ng of each VSG PCR product using the Nextera XT DNA Library Prepa-ration Kit (Illumina, FC-131-1096); this was done according to the manufacturer's protocol with the exception of the final cleanup step which was performed using 1X Mag-Bind beads. Single-end 100bp sequencing was performed on an Illumina HiSeq 2500. Raw data are available in the NCBI Sequence Read Archive under accession number PRJNA751607.

VSG-seq analysis of *T. b. gambiense* and *T. b. rhodesiense* sequencing libraries

For the analysis of both *T. b. gambiense* (VSG-seq preparations) and *T. b. rhodesiense* (traditional mRNA sequencing library preparations; sequences were obtained from ENA, accession numbers PRJEB27207 and PRJEB18523) raw reads were processed using the VSG-seq pipeline available at https://github.com/mugnierlab/VSGSeqPipeline. Briefly, *VSG* transcripts were assembled *de novo* from quality- and adapter-trimmed reads for each sample (patient or patient replicate) from raw reads using Trinity (version

5.26.2) [43]. Contigs containing open reading frames (ORFs) were identified as previously described [30]. ORF-containing contigs were compared to Lister427 and EATRO1125 *VSGs* as well as a collection of known contaminating non-*VSG* sequences. Alignments to *VSGs* with an E-value below $1x10^{-10}$ that did not match any known non-*VSG* contaminants were identified as *VSG* transcripts. For *T. b. gambiense* replicate libraries, *VSG* ORFs identified in any patient replicate were consolidated into a sole reference genome for each patient using CD-HIT (version 4.8.1)[44] with the following arguments: -d 0 -c 0.98 -n 8 -G 1 -g 1 -s 0.0 -aL 0.0. Final *VSG* ORF files were manually inspected. Two *T. b. gambiense* patient *VSG*s (Patients 11 and 13) showed likely assembly errors. In one case a *VSG* was duplicated and concatenated, and in another two *VSGs* were concatenated. These reference files were manually corrected (removing the duplicate or editing annotation to reflect two *VSGs* in the concatenated ORF) so that each *VSG* could be properly quantified. *VSG* reference databases for each patient are available at https://github.com/mugnierlab/Tbgambiense2021/. For *T. b. gambiense,* reads from each patient replicate were then aligned to that patient's consolidated reference genome using Bowtie with the parameters *-v 2 -m 1 -S* (version 1.2.3)[45] . For *T. b. rhodesiense,* each patient's data was aligned to its own *VSG* ORF assembly. RPKM values for *VSG* expression in each sample were generated using MULTo (version 1.0) [46], and the percentage of parasites in each population expressing a *VSG* was calculated as described previously [30]. For *T. b. gambiense* samples, we included only *VSGs* with an expression measurement above 1% in two or more patient replicates in our analysis. For *T. b. rhodesiense* samples, we included only *VSGs* with expression >0.01%. To compare *VSG* expression between patients, despite the different reference genomes used for each patient, CD-HIT was used to cluster *VSG* sequences with greater than 98% similarity among patients, using the same parameters as were used for consolidation of reference *VSG* databases before alignment. Each unique *VSG* cluster was given a numerical ID (e.g. Gambiense #) and the longest sequence within each group was chosen to represent the cluster. Clusters representing TgSGP and SRA were manually removed from the expressed *VSG* sets before analysis. R code used for analysis of resulting data and the generation of figures is available at https://github.com/mugnierlab/Tbgambiense2021/.

Analysis of VSG N-terminal Domains

Genomic *VSG* sequences

The *VSG* repertoires of *T. b. brucei* Lister427 ("Lister427_2018" assembly), *T. b. brucei* TREU927/4 and *T. b. gambiense* DAL972 were taken from TriTrypDB (v50). The *T. b. brucei* EATRO 1125 VSGnome was used for analysis of the EATRO1125 *VSG* repertoire (vsgs_tb1125_nodups_atleast250aas_pro.txt, available at https://tryps.rockefeller.edu/Sequences.html or GenBank accession KX698609.1 - KX701858.1). Likely VSG N-termini were identified as predicted proteins with significant similarity (e-value ≤ 10^{-5}) to hidden Markov models (HMMs) of aligned type A and B VSG N-termini taken from [15]. VSG sequences from other strains (except those generated by VSG-seq) were taken from the analysis in Cross, et al. [15].

298
299 N-terminal domain phylogenies
300 Phylogenies of VSG N-termini based on unaligned sequence similarities were
301 constructed using the method described in [47] and used previously to classify VSG
302 sequence [15]. N-termini were extracted as all predicted protein sequence up to the C-
303 terminal end of the bounding envelope of the match to either type-A or type-B HMM
304 (whichever was longer). A matrix of similarities between all sequences was constructed
305 from normalized transformed BLASTp scores as in Wickstead, et al. [47] and used to
306 infer a neighbor-joining tree using QuickTree v1.1 [48]. Trees were annotated and
307 visualized in R with the package APE v5.2 [49].
308
309 HMM
310 For N-terminal typing by HMM, we used a python analysis pipeline available at
311 (https://github.com/mugnierlab/find_VSG_Ndomains). The pipeline first identifies the
312 boundaries of the VSG N-terminal domain using the type A and type B HMM profiles
313 generated by Cross *et al.* which includes 735 previously-typed VSG N-terminal domain
314 sequences [15]. N-terminal domains are defined by the largest envelope domain
315 coordinate that meets e-value threshold ($1x10^{-5}$, --domE 0.00001). In cases where no
316 N-terminal domain is identified using these profiles, the pipeline executes a “rescue”
317 domain search in which the VSG is searched against a ‘pan-VSG’ N-terminus profile we
318 generated using 763 previously-typed VSG N-terminal domain sequences. This set of
319 VSGs includes several *T. brucei* strains and/or subspecies: Tb427 (559), TREU927
320 (138), *T. b. gambiense* DAL972 (28), EATRO795 (8), EATRO110 (5), *T. equiperdum*
321 (4), and *T. evansi* (21). The N-terminal domain type of these VSGs were previously
322 determined by Cross et. al (2014) by building neighbor-joining trees using local
323 alignment scores from all-versus-all BLASTp similarity searches [15]. Domain
324 boundaries are called using the same parameters as with the type A and B profiles.
325
326 After identifying boundaries, the pipeline extracts the sequence of the N-terminal
327 domain, and this is searched against five subtype HMM profiles. To generate N-terminal
328 domain subtype HMM profiles, five multiple sequence alignments were performed using
329 Clustal Omega [50] with the 763 previously-typed VSG N-terminal domain sequences
330 described above; each alignment included the VSG N-terminal domains of the same
331 subtype (A1, A2, A3, B1, and B2). Alignment output files in STOCKHOLM format were
332 used to generate distinct HMM profiles for type A1, A2, A3, B1, and B2 VSGs using the
333 pre-determined subtype classifications of the 763 VSGs using HMMer version 3.1b2
334 [51]. The number of sequences used to create each subtype profile ranged from 75 to
335 211. The most probable subtype is determined by the pipeline based on the highest
336 scoring sequence alignment against the subtype HMM profile database when HMMscan
337 is run under default alignment parameters. The pipeline generates a FASTA file
338 containing the amino acid sequence of each VSG N-terminus and a CSV with
339 descriptions of the N-terminal domain including its type and subtype.
340
341 Network graph
342 N-terminal network graphs were made using VSG N-terminal domains from TriTrypDB
343 Lister427_2018 and *T. b. gambiense* DAL972 (v50) VSG sets described above, and the

T. b. gambiense and *T. b. rhodesiense* VSG N-termini which met our expression thresholds. Identified N-terminal domains were then subjected to an all-versus-all BLASTp. A pairwise table was created that includes each query-subject pair, the corresponding alignment E-value, and N-terminal domain type of the query sequence if previously typed in Cross, et al. [15]. Pseudogenes and fragments were excluded from the Lister427_2018 reference prior to plotting by filtering for *VSG* genes annotated as pseudogenes and any less than 400 amino acids in length, as the remaining sequences are most likely to be full length VSG. Network graphs were generated with the igraph R package[52] using undirected and unweighted clustering of nodes after applying link cutoffs based on E-value < 10^{-2}. The leading eigenvector clustering method [53] was used to detect and assign nodes to communities based on clustering (cluster_leading_eigen() method in igraph).

Analysis of VSG C-terminal Domain Types

VSG C-termini were extracted from expressed *T. b. gambiense VSGs*, *T.b. gambiense* DAL972 (v50), and 545 previously-typed VSG C-termini from the Lister 427 strain using the C-terminal HMM profile generated by Cross et al.[15], and the same HMMscan parameters as for N-termini (E-value < $1x10^{-5}$; largest domain based on envelope coordinates). An all-vs-all BLASTp was performed on these sequences, and network graphs were generated in the same manner as the N-terminal network graphs. Links were drawn between C-termini with a BLASTp E-value $\leq 1x10^{-3}$. The leading eigenvector method for clustering [53] was used to detect and assign nodes to communities based on clustering (cluster_leading_eigen() method in igraph).

Results

Parasites in gHAT patients express diverse sets of VSGs

To investigate *VSG* expression in natural human infections, we performed VSG-seq on RNA extracted from whole blood collected from twelve human African trypanosomiasis patients from five locations in the Kwilu province of the Democratic Republic of Congo (Fig 1A). The relative parasitemia of each patient was estimated by SL-QPCR [54], and the number of parasites after mAECT on buffy coat was estimated for all patients except patient 29 (Table 1). RNA extracted from 2.5 mL of whole blood from each patient was used to prepare libraries for VSG-seq. *T. brucei* RNA was amplified from host/parasite total RNA using a primer against the *T. brucei* spliced leader sequence and an anchored oligo-dT primer. The resulting trypanosome-enriched cDNA was then used as a template to amplify *VSG* cDNA. *VSG* amplicons were then submitted to VSG-seq sequencing and analysis. To determine whether a *VSG* was expressed within a patient, we applied the following stringent cutoffs:

1) We conservatively estimated that each 2.5 mL patient blood sample contained a minimum of 100 parasites. At this minimum parasitemia, a single parasite would represent 1% of the population (and consequently ~1% of the parasite RNA in a sample). As a result, we excluded all *VSGs* expressed by <1% of the population as estimated by VSG-seq.
2) We classified *VSGs* as expressed if they met the expression cutoff in at least two of three technical library replicates.

1112 unique *VSG* open reading frames were assembled *de novo* in the patient set and 44 met our expression criteria. Only these 44 *VSGs*, which we will refer to as "expressed *VSGs"* in these patient samples, were considered in downstream analysis, except when otherwise noted. TgsGP, the VSG-like protein which partially enables resistance to human serum in *T. b. gambiense* [55], was assembled in samples from patients 2, 11, 13, and 17, and met expression threshold in patients 2, 11, and 17. The absence of this transcript in most samples is likely a result of the low amount of input material used to prepare samples. Notably, none of the expressed *VSGs* shared similarity with any *VSGs* in the *T. b. gambiense* DAL972 genome or the diagnostic VSGs LiTat 1.3, LiTat 1.5 and LiTat 1.6.

At least one *VSG* met our expression criteria in each patient, and in most cases multiple *VSGs* were detected. The highest diversity was observed in patient 2, with 14 *VSGs* expressed (Fig 1B, Supplemental Figure 1). We observed a correlation between parasitemia as estimated by QPCR and number of *VSGs* (Supplemental Figure 2), suggesting that these samples do not reflect the full diversity of each population. Nevertheless, two *VSG* were shared between patients: *VSG* 'Gambiense 195' was expressed in both patient 12 and patient 17 from Village C, and *VSG* 'Gambiense 38' was expressed in patient 12 from Village C and patient 23 from Village D which are 40 kilometers apart (Fig 1C).

Patient	Location	Est. parasites in 500µL buffy coat	mean SL-RNA Ct	Plasma CATT end dilution	WBC	Parasites in CSF	Stage
1	Village A	>50	22.155	≥32	1	-	First
2	Village A	>50	19.020	≥32	6	-	Early 2nd
3	Village A	2-5	28.780	≥32	6	-	Early 2nd
11	Village C	>50	22.030	4	9	-	Early 2nd
12	Village C	6-20	25.430	≥32	6	-	Early 2nd
13	Village C	6-20	26.635	16	12	-	Early 2nd
17	Village C	21-50	24.495	≥32	13	-	Early 2nd
19	Village C	1	28.245	8	7	-	Early 2nd
23	Village D	6-20	27.085	≥32	2	-	First
29	Village B	-	28.320	≥32	3	-	First
30	Village B	>50	22.960	≥32	694	+	Severe 2nd
33	Village E	1	32.385	≥32	2	-	First

Table 1. Patient stage and parasitemia data. For staging, the following definitions were used: First: 0-5 WBC/µl, no trypanosomes in CSF. Second: >5 WBC/µl or trypanosomes in CSF. (with early 2nd 6-20 WBC/µl and no trypanosomes in CSF; severe 2nd: >100 WBC/µl). WBC: white blood cells.

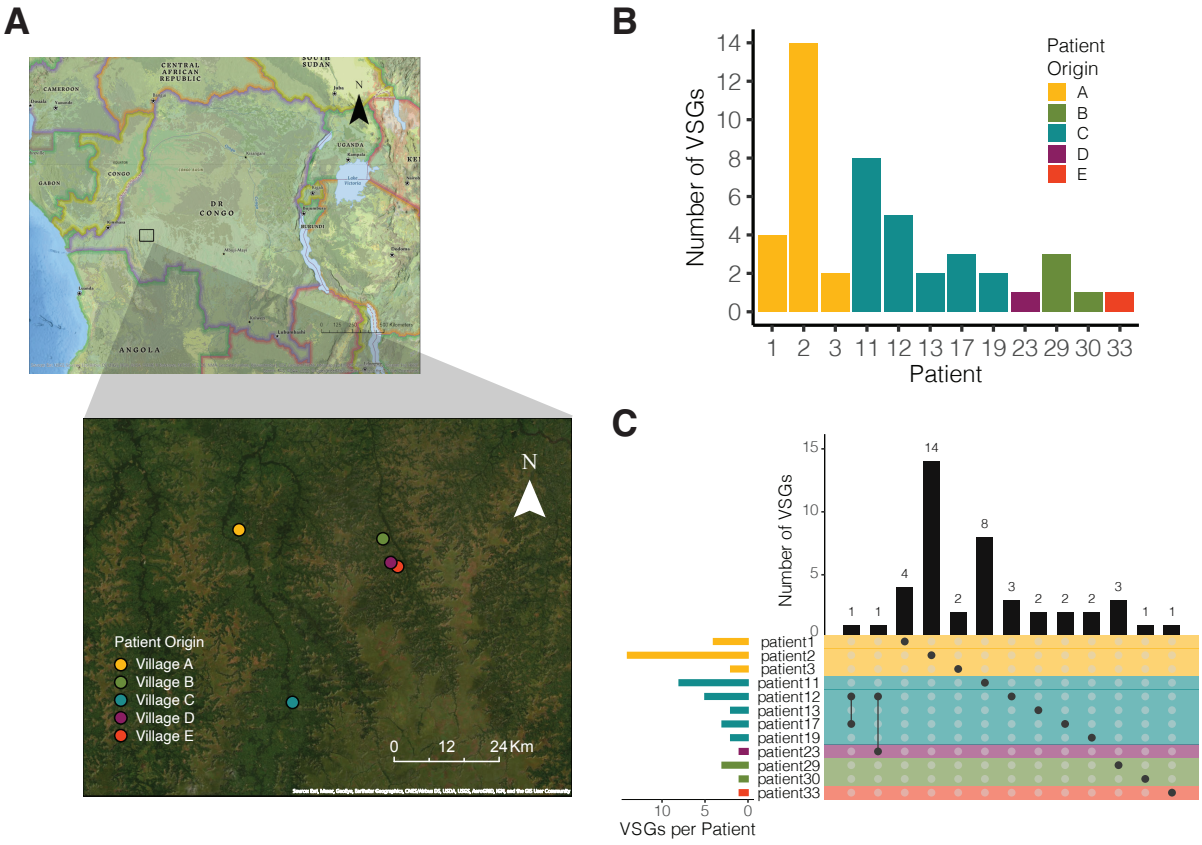

Figure 1. Parasites isolated from gHAT patients express multiple *VSGs*. (A) Map showing the location of each patient's home village. Maps were generated with ArcGIS® software by Esri, using world imagery and National Geographic style basemaps. (B) Graph depicting the

427 total number of *VSGs* expressed in each patient. (C) The intersection of expressed *VSG* sets in
428 each patient. Color indicates patient origin.

429

430 **Natural *T. b. gambiense* infections show a strong bias towards expression of type**
431 **B VSG**
432
433 To further characterize the set of expressed *VSGs* in these samples, we sought a fast
434 and unbiased method for determining the type and subtype of each VSG's N-terminal
435 domain. We evaluated two approaches. The first approach was to create a bioinformatic
436 pipeline to determine each N-terminal domain subtype, using HMM profiles we created
437 for each subtype using sets of N-terminal domains previously typed by Cross *et al.* [15].
438 The second approach was to create a BLASTp network graph based on a previously
439 published method [56] where the N-terminal subtype of a VSG is determined by the set
440 of VSGs it clusters with, and clusters are identified using the leading eigenvector
441 method [53]. We used each approach to determine the N-terminal subtype of each
442 expressed *VSG* in our patient sample dataset along with 863 VSG N-termini from the
443 Lister 427 genome. We compared these results to either existing N-terminal
444 classification (for Lister 427 VSGs) or classification based on position in a newly-
445 generated BLASTp-tree[15] (for *T. b. gambiense* VSGs; Figure 2A). Both the new HMM
446 profile and BLASTp network graph approaches generally recapitulated previous VSG
447 classification based on BLASTp-tree, with all three methods agreeing 93.7% of the time
448 (Figure 2B). The HMM pipeline method agreed with BLASTp-tree typing for all patient
449 VSGs, while the network graph approach agreed for 43/44 VSGs (Figure 2B,
450 Supplemental Fig 3, Supplemental Table 1) [15]. It is not surprising that the HMM
451 pipeline would better reflect the results of the BLASTp-tree method, as the N-terminal
452 subtype HMM profiles were generated using VSGs classified by this method. Based on
453 these data, we determined the HMM method is a fast and accurate method for
454 determining the N-terminal domain types of unknown VSGs.
455
456 Our N-terminal domain typing pipeline identified the domain sequence and type for all
457 44 patient VSGs (Fig 2C). 82% of the expressed *T. b. gambiense* VSGs had type B N-
458 terminal domains, and within each patient 50% or more of expressed *VSG* were type B.
459 This bias was not restricted to highly expressed *VSGs*, as 74.5% of all assembled *VSG*
460 (813 of 1091 classifiable to an N-terminal subtype) were also type B. This observation
461 motivated further investigation into the expressed N-terminal domains in infections by
462 other *T. brucei* subspecies.
463

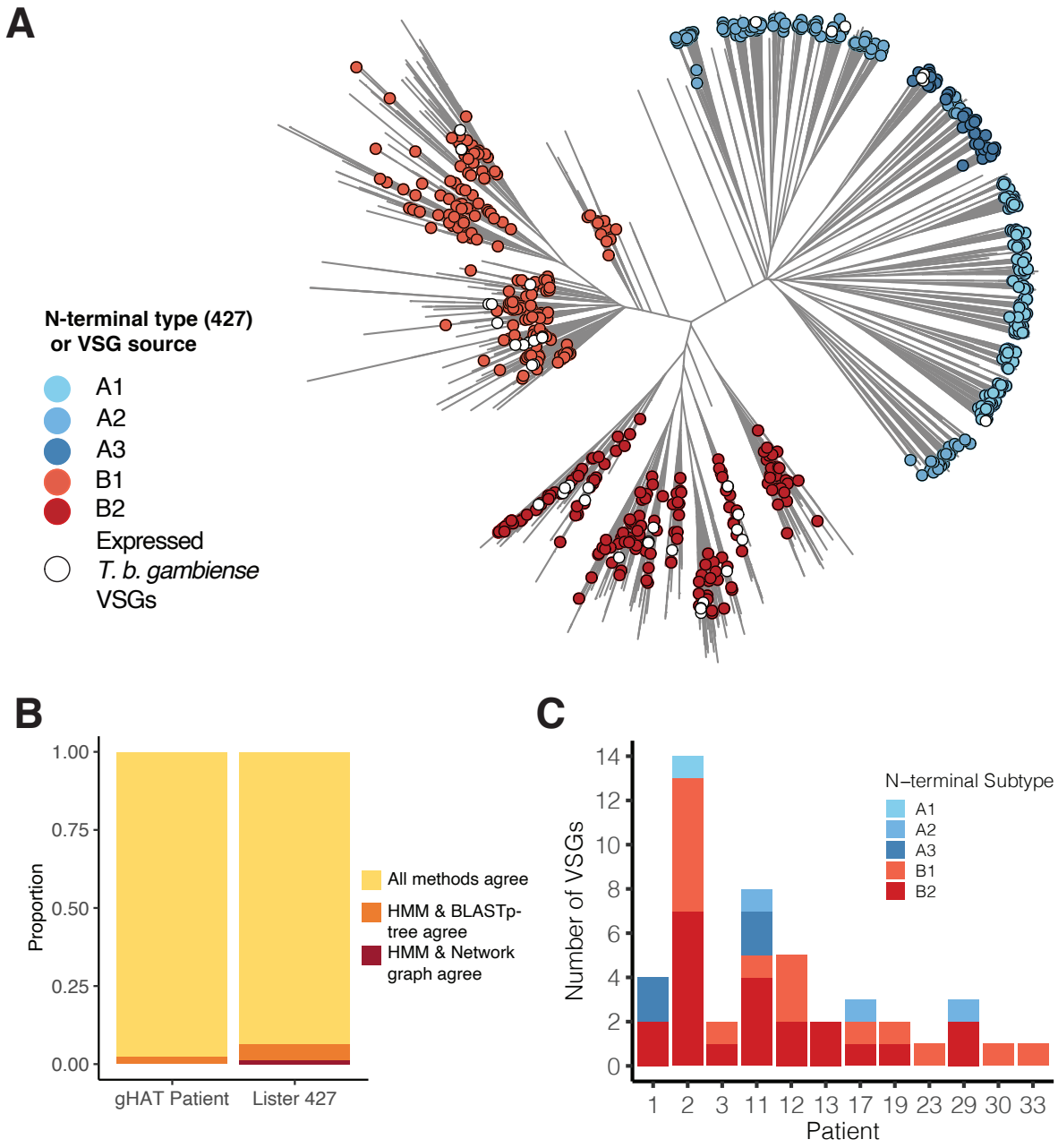

Figure 2. *T. b. gambiense* samples show a bias towards expression of type B VSG. (A) Visualization of relatedness between N-terminal domain peptide sequences inferred by Neighbor-Joining based on normalized BLASTp scores. Legend indicates classification by HMM pipeline (for Lister 427 VSGs, to highlight agreement between the two methods), or by subspecies for *VSGs* expressed in patients. (B) Agreement between three VSG typing methods for Lister 427 VSG set and the expressed *T. b. gambiense* patient VSG set. (C) N-terminal domain subtype composition of expressed *T. b. gambiense VSGs* as determined by HMM analysis pipeline.

Type B VSG bias is not observed in natural *T. b. rhodesiense* infection.

To determine whether the bias towards type B VSGs was unique to *T. b. gambiense* infections, we analyzed RNA-seq data from a published study measuring gene expression in the blood and cerebrospinal fluid (CSF) of *T.b. rhodesiense* patients in Northern Uganda [57]. These libraries were prepared conventionally after either rRNA-depletion for blood or poly-A selection for CSF samples. We analyzed only those samples for which at least 10% of reads mapped to the *T. brucei* genome. Raw reads from these samples were subjected to the VSG-seq analysis pipeline, and because the estimated parasitemia of these patients was much higher than our *T.b. gambiense* study, we adjusted our expression criteria accordingly to 0.01%, the published limit of detection of VSG-seq [30]. Using this approach, we identified 77 unique *VSG* sequences across all blood and CSF samples (Fig 3A, Supplemental Figure 4). SRA, the VSG-like protein that confers human serum resistance in *T. b. rhodesiense* [58], was expressed in all patient samples.

The HMM pipeline was able to determine types for 74 of these VSG sequences; the remaining appeared to be incompletely assembled, presumably due to insufficient read depth from their low level of expression. In each patient, multiple *VSGs* assembled and a large proportion were expressed in multiple patients (Fig 3B), in line with our observations in experimental mouse infections. Although the majority of VSGs detected in these patients were type B (57%), this VSG type was much less predominant than in *T. b. gambiense* infection (Fig 3C). Interestingly, there was no overlap in expressed *VSGs* in the blood and CSF of patient 71, the only patient for which both blood and CSF data were available for analysis, potentially indicating that different organs or body compartments harbor different sets of VSGs.

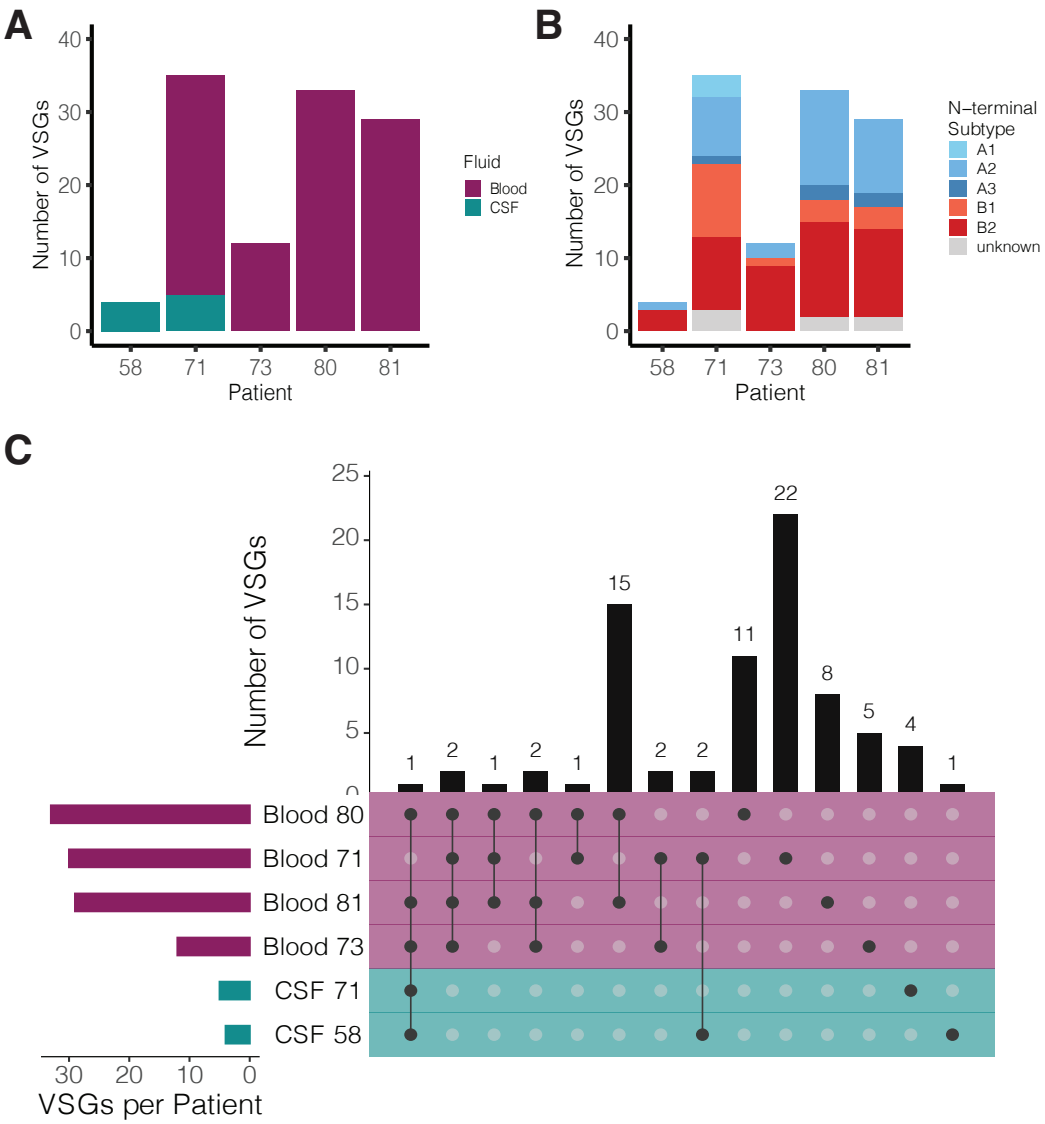

Figure 3. *T. b. rhodesiense* samples reveal diverse *VSG* expression, but little N-terminal type bias. (A) The total number of expressed *T. b. rhodesiense VSG* in each patient and sample type. Bar color represents sample type from which RNA was extracted. (B) N-terminal domain subtype composition of all expressed *VSGs*. (C) Intersections of *VSGs* expressed in multiple infections. Color represents the sample type.

The predominant VSG N-terminal type fluctuates over time during experimental *T. b. brucei* infection

One explanation for the bias towards type B VSG in *T. b. gambiense* could be that VSG type fluctuates over time. This is plausible because patient samples only represent a single moment during infection, and *T. b. gambiense* samples are more likely to be obtained at a later stage of infection than *T. b. rhodesiense*. To investigate whether a

predominance of type B VSGs could be a feature of the chronic nature of *T. brucei gambiense* infection, we took advantage of our published VSG-seq analysis of parasites isolated from mice infected with the *T.b. brucei* EATRO1125 strain. Blood was collected over time during this study, providing data from days 6/7, 12, 14, 21, 24, 26, and 30 post infection in all four mice, and from days 96, 99, 102, and 105 in one of the four mice (Mouse 3). Of 192 unique VSGs identified between days 0-30 and 97 VSGs identified between days 96-105,190 and 93 VSGs were typed by the python HMM pipeline, respectively. The remaining VSGs were incompletely assembled by Trinity. Our analysis of VSG types over time revealed that the predominantly expressed N-terminal domain type fluctuates between type A and type B throughout the early stages of infection as well as in extended chronic infections (Fig 4). Parasitemia did not correlate with either the diversity of *VSG* expression or N-terminal domain type predominance (Supplemental Fig 3). Because all patient samples were collected from a single timepoint, it remains unclear whether the predominant N-terminal type fluctuates in human infections over time as it does in mice.

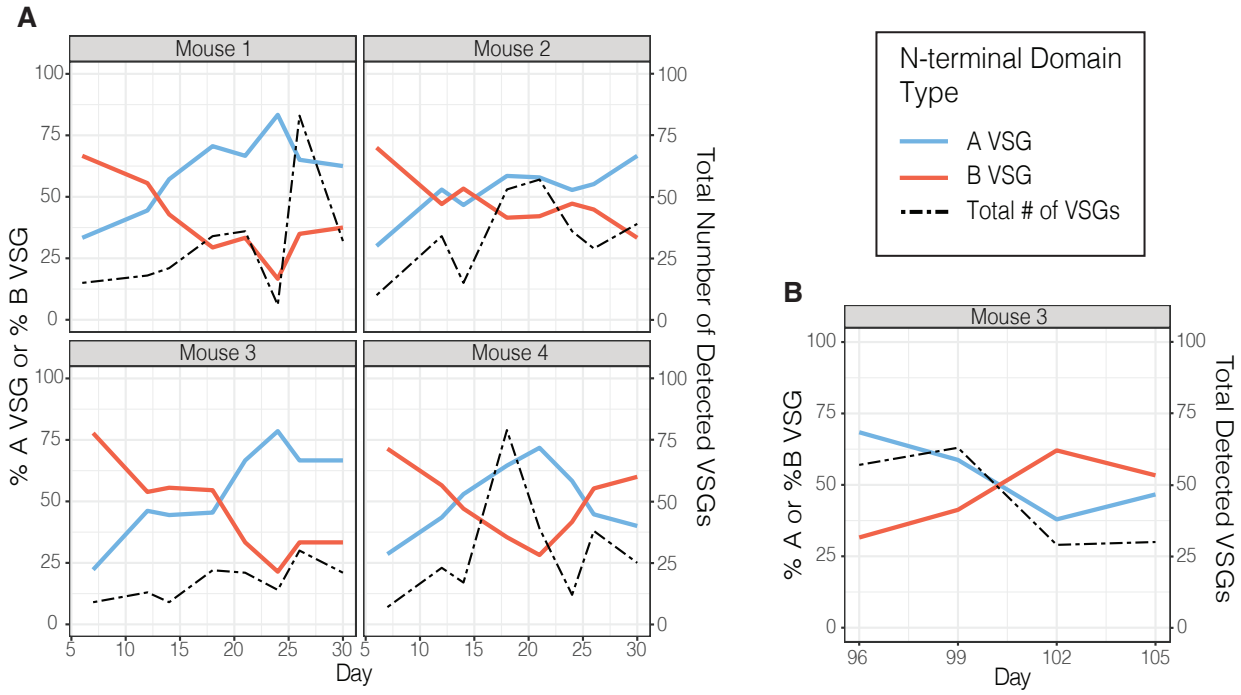

Figure 4. VSG N-terminal type composition fluctuates over the course of infection in mice. Proportions of N-terminal domain types expressed in *T. b. brucei* infected mice over time. Total number of identified VSGs is represented by the black dotted line. A) N-terminal type composition days 0-30. B) Type composition days 96-105.

The composition of the genomic VSG repertoire is reflected in expressed VSG N-terminal domain types

Another source for bias in expressed VSG type is the composition of the genomic *VSG* repertoire. We were only able to make a direct comparison between the genomic and expressed *VSG* repertoire for EATRO1125 mouse infections, as the 'VSGnome' for this strain has been sequenced. This analysis revealed that, although the predominant N-terminal VSG type fluctuates during infection, the expressed *VSG* repertoire generally reflects the composition of the genomic repertoire (chi-squared p = 0.0515, Figure 5A).

Unfortunately, the full repertoire of *VSGs* encoded by most trypanosome strains is unknown, so such a direct comparison is impossible for *T. b. gambiense* and *T. b. rhodesiense* patient samples. The *T. b. gambiense* DAL972 reference genome lacks most of the genomic regions containing the majority of *VSGs* (haploid arrays, expression sites, and minichromosomes), and there is no publicly available *T. b. rhodesiense* reference assembly. However, there is no significant difference in VSG type frequency comparing the expressed *T. b. rhodesiense* set to the closely related and near-complete *T. b. brucei* Lister 427 repertoire [59] (chi-squared p-value = 0.2422) (Fig 5B). Similarly, the proportion of N-terminal domains identified in the *T. b. gambiense* patient samples is not statistically different from the incomplete *T. b. gambiense* DAL972 genomic repertoire (chi-squared p-value = 0.0575) (Fig 5B). Both *T. b. gambiense* patient VSG (chi-squared p-value = 2.413e-4) and the 54 VSGs identified in *T. b. gambiense* DAL972 (chi-square p-value = 0.0301) have A and B type frequencies that differ significantly from Lister427. Though these results should be interpreted with caution given the limitations of the reference genomes being used, they generally suggest that the underlying genomic *VSG* repertoire of *T. b. gambiense* differs from other subspecies in its N-terminal type composition.

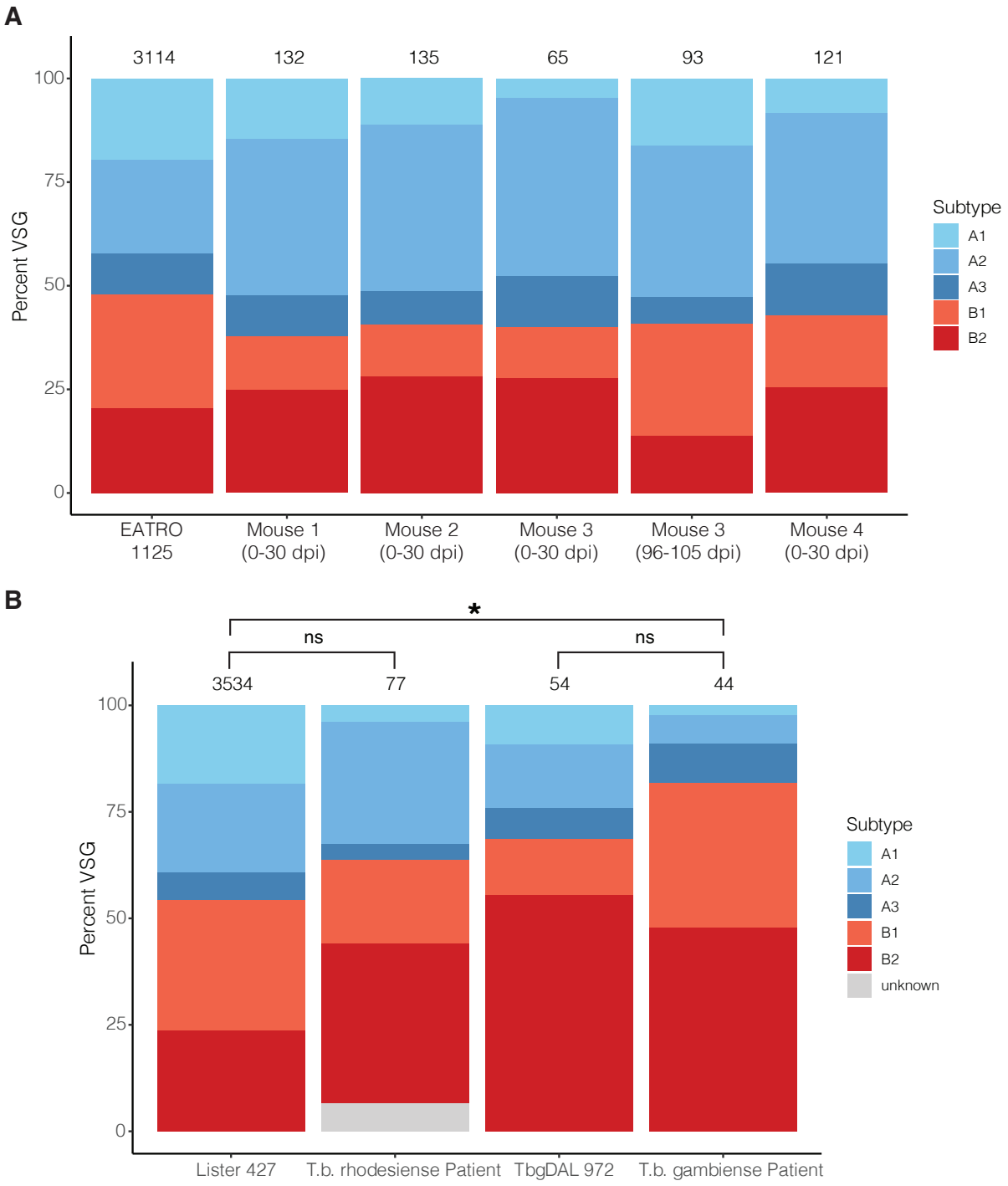

Figure 5. VSG expression reflects the genomic VSG repertoire of the infecting parasites. (A) Columns show the proportion of VSG types identified in each mouse infection over all time points. Total number of unique VSG sequences displayed above column. Mouse infections were initiated with *T.b. brucei* strain EATRO 1125. (B) A comparison of the frequencies of type A and B VSGs expressed in patients and those present in Lister 427 and DAL972 reference genomes.

T.b. gambiense expressed VSG C-terminal domains show a bias for type 2 domains

In addition to examining N-terminal types in our *T. b. gambiense* dataset, we also examined expressed VSG C-termini. Previous studies defined six C-terminal types, although resolution of these types in larger VSG sets has been difficult due to the high level of similarity among VSG C-termini [15,56]. In line with previous observations, a BLASTp-tree analysis of assembled *T.b. gambiense* C-terminal domains revealed frequent sequence similarity between expressed C-terminal types but did not provide sufficient resolution to confidently assign types (Fig 6A).

To supplement this analysis, we also performed a network graph analysis. Although this method had previously performed poorly in resolving VSG C-termini [56], using the leading eigenvector clustering method [53] to define community membership within the graph allowed a faithful reconstitution of the C-terminal types previously determined by BLASTp tree analysis. Using this approach, we were able to tentatively assign C-terminal domain types to the *T. b. gambiense* VSGs (Fig 6B). Most patient C-terminal domain types were type 2, while the remaining largely fell into the type 1 category. Only one type 3 C-terminus was identified in the patient set. Although there are very few VSG C-termini available in the *T. b. gambiense* DAL972 genome, these sequences show a predominance of types 3 and 5, while the genomic repertoire of C-termini in Lister427 shows roughly equivalent representation of types 1, 2, and 3. Unlike *T. b. gambiense* N-termini, the expressed C-termini were more restricted than the sets of C-termini apparently available in the *T. b. gambiense* DAL972 or *T. b. brucei* Lister427 genomes (Fisher's exact test, p-value < $1x10^{-5}$). In line with previous observations, we saw no evidence of domain exclusion: a C-terminal domain of one type could be paired with any type of N-terminal domain (Fig 6E)[20]. As observed in our analysis of expressed N-termini, C-terminal domain types were not correlated to geographical origin (Fig 6F). Overall, these data suggest that, like N-termini, expressed VSG C-termini are also biased towards certain C-terminal types. Unlike N-termini, however, C-terminal types expressed in *T. b. gambiense* infection may not reflect the composition of the parasite's genomic repertoire.

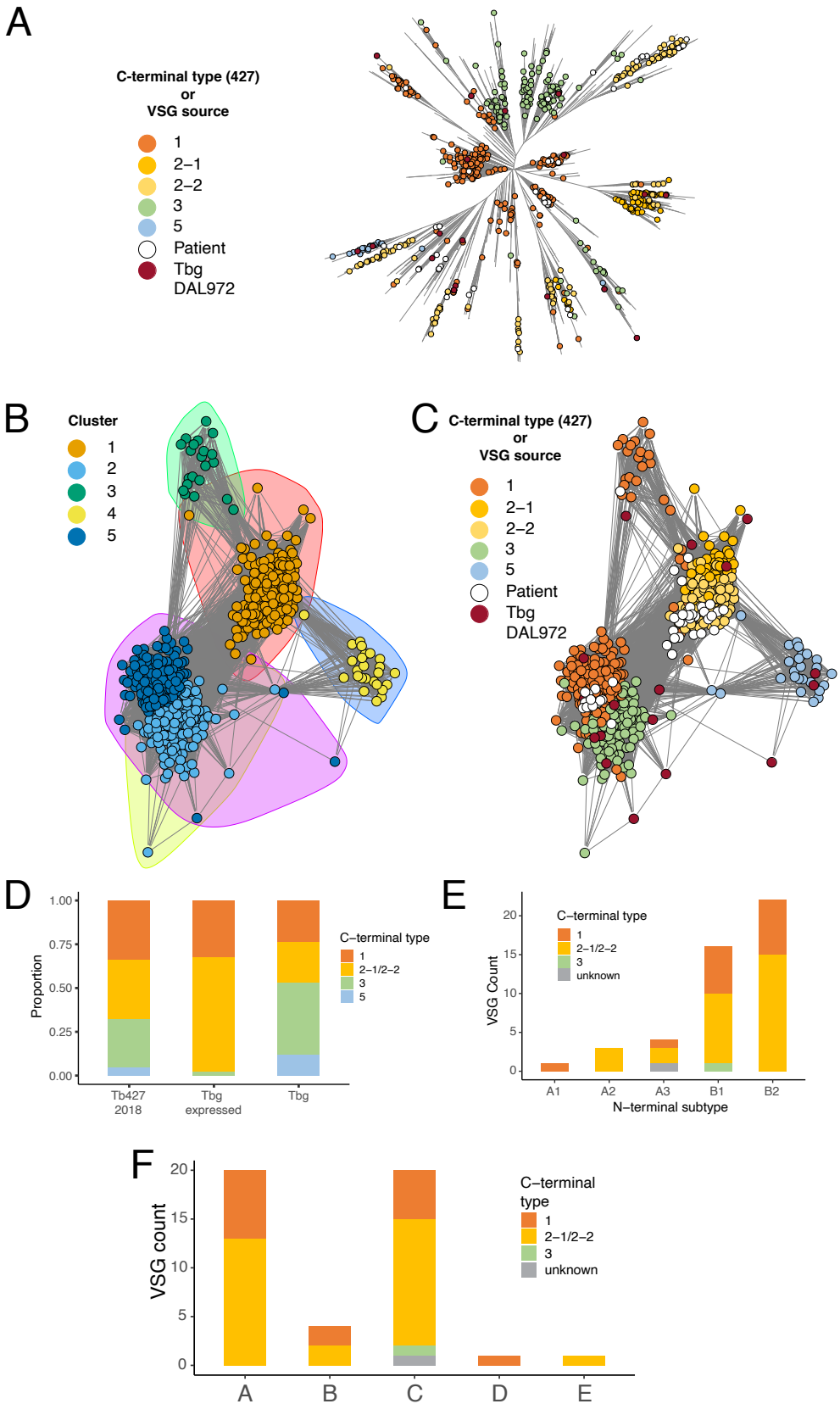

Figure 6. Expressed VSG C-termini are primarily type 1 and type 2. A) BLASTp tree of C-terminal domains. Points are colored based on previously-determined C-terminal type from Cross et al., or by the source of the sequence (genomic or expressed) for *T. b. gambiense VSGs*. B) Network plot showing peptide sequence relatedness between C-terminal domains in *T. b. gambiense* expressed VSGs. Each point represents a VSG C-terminus; a link was drawn between points if BLASTp e-value was less than $1x10^{-3}$. Points are colored by cluster determined by the clustering algorithm. Clusters are also indicated by shaded circles. C) Same network plot as in B, but colored by previously-determined C-terminal type from Cross et al., or by source for unclassified genomic or expressed *VSGs*. D) VSG C-terminal types, based on cluster assignment visualized in panel B, in genomic and expressed *VSG* sets. E) Pairing of C- and N-termini in *T. b. gambiense* patients. F) C-termini detected in each patient village.

Discussion

African trypanosomes evade the host adaptive immune response through a process of antigenic variation, where parasites switch their expressed *VSG* [60]. The genome of *T. brucei* encodes a large repertoire of *VSG* genes, pseudogenes, and gene fragments, and can be extended continuously through recombination to form entirely novel "mosaic" *VSGs* [17]. While antigenic variation has been studied extensively in culture and in animal models of infection, our understanding of the process in natural infections, particularly human infection, is limited. Most experimental mouse infections are sustained for weeks to months, while humans and large mammals may be infected for several months or even years. Additionally, laboratory studies of antigenic variation almost exclusively use *T. b. brucei*, a subspecies of *T. brucei* that, by definition, does not infect humans.

The primary hurdle to exploring antigenic variation in nature has been technical: it is difficult to obtain sufficient parasite material for analysis. This is especially true for infection with *T. b. gambiense,* which often exhibits extremely low parasitemia. VSG-seq, which relies on PCR and requires very small amounts of material for analysis, provides a new tool for exploring *VSG* expression in natural human infections. Here we have demonstrated the feasibility of VSG-seq to analyze *VSG* expression in RNA samples isolated directly from HAT patients. Our analyses show that the diversity seen in mouse models of infection is mostly recapitulated in natural infection, but that there may be unique aspects of antigenic variation in *T. b. gambiense* that can only be explored by studying natural infections.

In our previous analysis of mouse infections, the most notable result was the diversity of *VSGs* expressed. Rather than a few *VSGs* expressed at a time, we saw many *VSGs* expressed simultaneously in the populations, confirming previous estimates of antigenic diversity in experimental mouse infection [17] and suggesting that the genomic *VSG* repertoire might be exploited very rapidly. In the study presented here, we detected several expressed *VSGs* in most *T. b. gambiense* samples. Although diversity in *T. b. gambiense* infection appeared lower overall, the correlation we observed between parasitemia and diversity in *T. b. gambiense* isolates specifically suggests that our sampling was incomplete. Indeed, in our analysis of *T. b. rhodesiense* infection (a more reasonable comparison to mouse infection given similar expression cutoffs and parasitemia), we observed diversity similar to or higher than what we have detected in *T. b. brucei* mouse infections. Moreover, *T. b. rhodesiense* patient CSF revealed another layer of diversity in *VSG* expression, with 5 *VSGs* expressed exclusively in this space. Overall, our analysis of *VSG* expression in *T. b. gambiense* and *T. b. rhodesiense* patients confirmed the long-held assumption that *VSG* diversity is a feature of natural infection.

While analyzing the sets of expressed *VSGs* in *T. b. gambiense* and *T. b. rhodesiense* infections, we found evidence for another feature of experimental infection that holds true in a natural host: hierarchical *VSG* expression. Both *in vitro* and *in vivo* studies have shown that *VSG* switching is not entirely stochastic but rather hierarchical, with

certain variants dominating expression in the parasite population in a reproducible order that appears to be independent of the starting *VSG* [17,31,32,61,62]. Switching hierarchy is hypothesized to be determined by multiple factors including homology, gene size, and genomic location. In the *T. b. gambiense* samples, we found two *VSGs* that met our detection threshold in multiple patients, and in *T. b. rhodesiense* a large proportion of expressed *VSGs* were shared among multiple patients. Given the large size of the genomic *VSG* repertoire, any overlap in expressed *VSG* repertoire is likely indicative of a semi-predictable hierarchy of switching and preference for the expression of certain *VSGs*.

Of the two shared *VSGs* we identified in the *T. b. gambiense* patients, one was identified in two patients from the same village, while the other was found in two patients from villages 40km apart. At this short distance, it is possible that the infecting parasites were genetically similar and thus this overlap simply reflects preference in switching. It would be interesting to investigate, however, whether preference for the expression of certain *VSGs* occurs even between parasites isolated at greater distances. Indeed, it has been shown that the sensitivity of serological tests for gHAT, which detect antibody against the LiTat 1.3 VSG, vary regionally, potentially due to differences in the underlying genomic or expressed *VSG* repertoire in circulating strains [63,64]. Along these same lines, none of our assembled *T. b. gambiense VSGs* from patients in the DRC shared significant similarity with those in the genome of DAL972, a parasite isolate from Côte d'Ivoire. This could suggest that there are geographic variations in *T. brucei VSG* repertoires. Similar variation has been observed in *var* gene repertoires of *Plasmodium falciparum* [65] and the *VSG* repertoire of *Trypanosoma vivax*, another African trypanosome [35]. A better understanding of such differences in *T. brucei*, if they exist, could lead to development of more sensitive HAT diagnostics.

To better understand the VSG proteins expressed in natural infections, we developed an HMM VSG typing pipeline that revealed an intriguing bias in *T. b. gambiense* infection towards type B VSGs that appears to be specific to *T. b. gambiense* patient samples. While small sample sizes and important differences between each *T. brucei* subspecies' dataset limit the conclusions that can be drawn, comparisons between these sets do suggest that the genomic *VSG* repertoire determines the distribution of VSG N-terminal types expressed during *T. brucei* infection and may account for the bias we have observed in *T. b. gambiense* patients.

Our analysis of experimental mouse infections suggests that while the predominant expressed N-terminal domain type fluctuates between type A and type B over time, even into advanced stages of infection, the repertoire expressed over the course of an infection generally reflects the composition of the genomic *VSG* repertoire of the infecting parasite strain. A direct comparison between the genomic *VSG* repertoire and the expressed *VSG* repertoire can be made for experimental *T. b. brucei* EATRO1125 infections, as the EATRO1125 VSGnome was generated from the same parasite strain used to initiate these infections. Such a direct comparison is impossible for patient samples. While the content of the 'core' *T. brucei* genome (containing the diploid, housekeeping genes) is similar enough among subspecies for resequencing projects to

be scaffolded using the TREU927 or Lister 427 reference genomes [59,66,67], it is not clear whether the *VSG* repertoires of subspecies (or even individual parasite strains [36]) share this degree of similarity. Although a near-complete VSGnome for any *T. b. rhodesiense* strain was not available, we chose to compare the makeup of *T. b. rhodesiense* expressed *VSGs* with the well-characterized genome of *T. b. brucei* Lister 427 [16], given the extreme similarity between *T. b. brucei* and *T. b. rhodesiense* [59]. Similarly, we compared expressed *VSGs* in *T. b. gambiense* patients to the limited set of *VSGs* in the *T. b. gambiense* DAL972 genome. In both cases, the distribution of N-terminal types expressed in infection was not significantly different from that of the genomic *VSG* repertoire to which the expressed *VSGs* were being compared. Taken together, these data support a model in which VSG types are drawn from the repertoire at roughly equal frequency to their representation in the genome, and that that the *T. b. gambiense VSG* repertoire may contain a larger proportion of type B VSG than its more virulent counterparts.

Another possibility we cannot rule out is that the gHAT samples are biased due to selection by the serological test used for diagnosis. Patients were screened for *T. b. gambiense* infection using the CATT, a serological test that uses parasites expressing VSG LiTat 1.3 as an antigen. LiTat 1.3 contains a type B2 N-terminal domain [63,64]. It is possible that patients infected with parasites predominantly expressing type B VSGs are more likely to generate antibodies that cross-react with LiTat1.3, resulting in preferential detection of these cases. In contrast, *T.b. rhodesiense* can only be diagnosed microscopically, removing the potential to introduce bias through screening. It remains to be investigated whether samples from patients diagnosed using newer screening tests, which include the invariant surface glycoprotein ISG65 and the type A VSG LiTat 1.5 [29], would show similar bias towards expression of type B VSGs.

Analysis of expressed VSG C-terminal domains in *T. b. gambiense* patients showed a bias towards C-terminal types 1 and 2. The diagnostic VSG LiTat1.3 contains a type 3 C-terminus, a C-terminal type which was underrepresented in the patient set. Therefore, it is unlikely that a bias in expressed C-terminal types is related to the screening method. Notably, the bias towards C-terminal types 1 and 2 was not reflected in the limited *VSG* repertoire of the DAL972 reference genome or the repertoire of the Lister 427 *T. b. brucei* reference genome. This could be related to the limited set of *VSG*s present in the DAL972 reference genome, or it could suggest a true bias in expression.

Could a bias towards certain VSG types, whether due to a difference in repertoire composition or expression preference, account for the chronic nature of gHAT? While the genomic *VSG* repertoire has been analyzed extensively in laboratory strains, little is known about how differences in VSG proteins relate to parasite biology or whether there could be biological consequences to the expression of specific VSG N- or C-terminal types. Type A *var* genes in *Plasmodium falciparum* infection have been shown to be associated with severe malaria [68–72], and similar mechanisms have been hypothesized to exist in *T. vivax* and *T. congolense* infections [33,35,73,74]. In *T. brucei,* several VSGs have evolved specific functions besides antigenic variation [74]. Recently, the first type B VSG structure was solved [75], revealing a unique *O*-linked

carbohydrate in the VSG's N-terminal domain. This modification was found to interfere with the generation of protective immunity in a mouse model of infection; perhaps structural differences between each VSG type, including patterns of glycosylation, could influence infection outcomes. Further research will be needed to determine whether the observed predominance of type B VSGs could influence the clinical presentation of *T. b. gambiense* infection.

Currently, it is unclear why this collection of gHAT patient isolates demonstrates a bias towards expression of certain VSG types. More research will be needed to determine whether the *T. b. gambiense VSG* repertoire contains a unique distribution of VSG types, whether these parasites preferentially express certain VSG types, and whether this bias could have functional consequences. What this study has shown, however, is that it is feasible to explore antigenic variation in natural infection and that, although mouse models do reflect the general dynamics of antigenic variation in natural *T. brucei* infection, unique biology remains to be uncovered by studying antigenic variation in its natural context.

Acknowledgments

We are very grateful to the patients without whom this work would not have been possible. We thank George Cross and Danae Schulz for comments on the manuscript. We would also like to thank Mary Gebhardt for help with GIS. The atlas of HAT is an initiative of the World Health Organization (WHO), jointly implemented with the Food and Agriculture Organization of the United Nations (FAO) in the framework of the Programme Against African Trypanosomosis (PAAT).

Supplement

Supplemental Table 1. Primer sequences.

Supplemental Table 2. gHAT patient distance matrix.

Supplemental Table 3. gHAT VSG expression data.

Supplemental Table 4. Tables comparing BLAST-tree, HMMscan, and network plot typing methods.

Supplemental Table 5. rHAT VSG expression data.

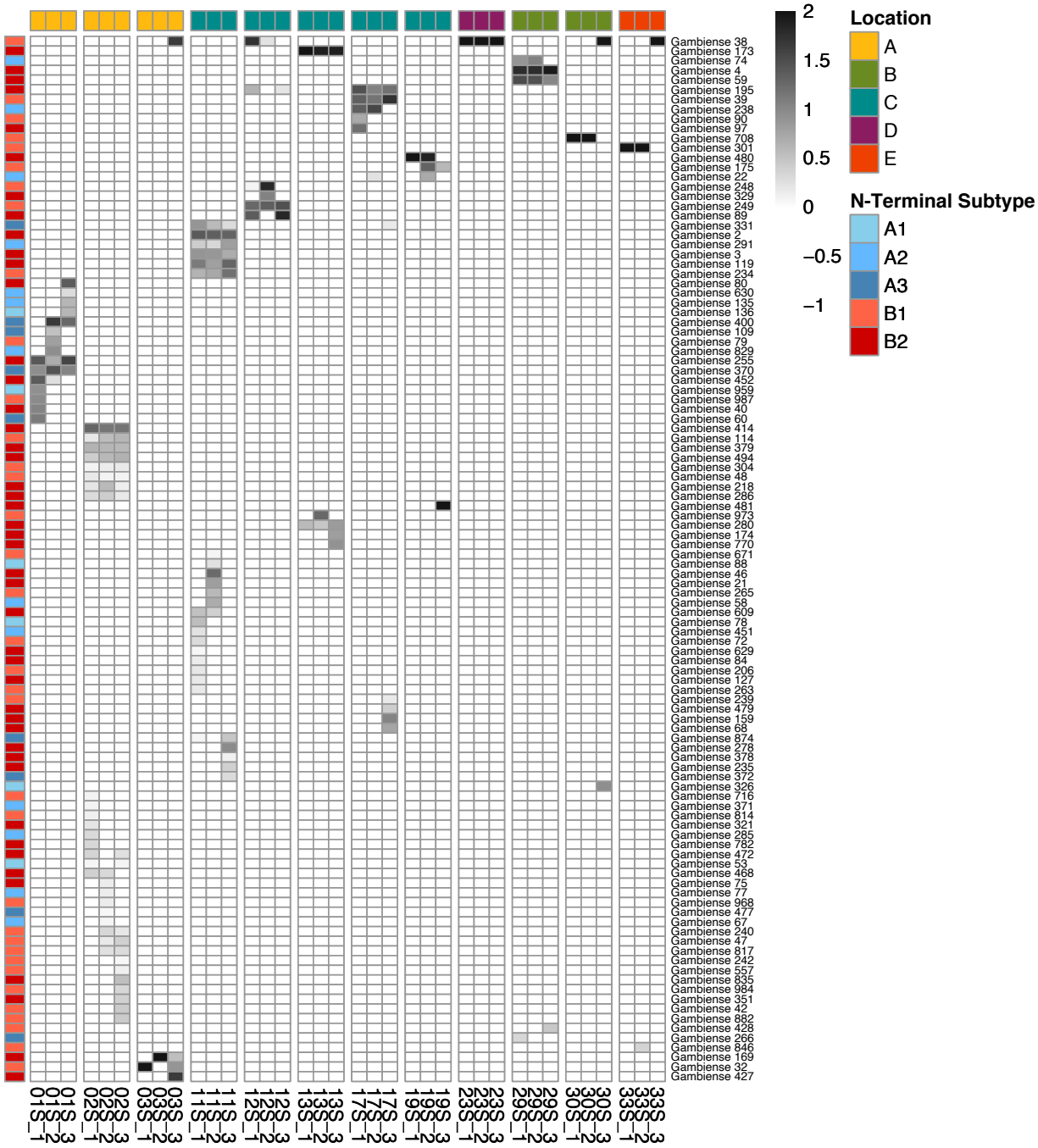

Supplemental Figure 1. Heatmap of all assembled *T.b. gambiense* patient VSGs

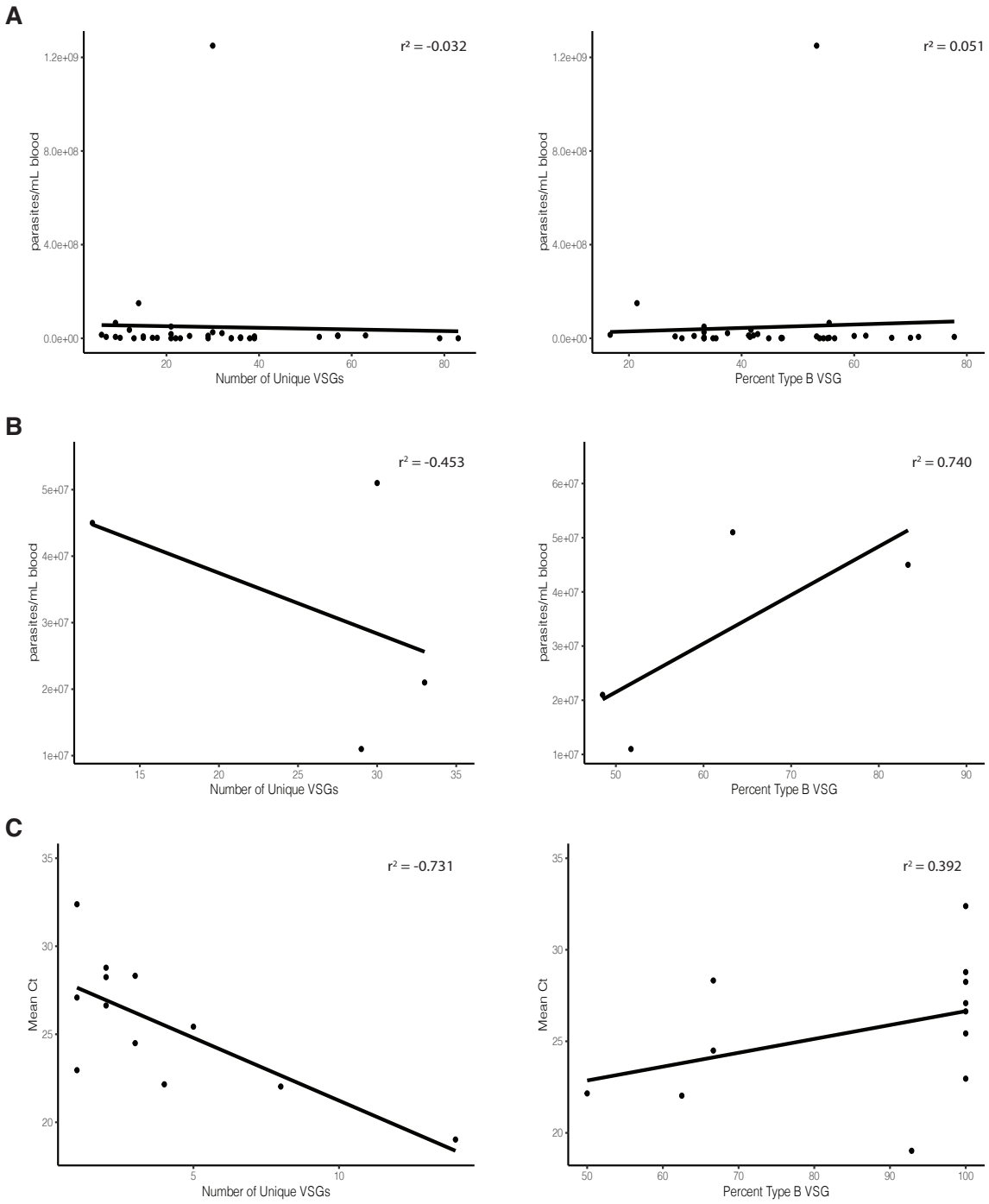

Supplemental Figure 2. Correlation between parasitemia and diversity and N-terminal type distribution. (A) Correlation plots for VSG diversity and percent of N-terminal domain type B for *T.b. brucei* infected mice from Mugnier et.al 2015. (B) Correlation plots for *T.b. rhodesiense* infected patients from Mulindwa et. al. 2018. (C) Correlation plots for *T.b. gambiense* infected patients.

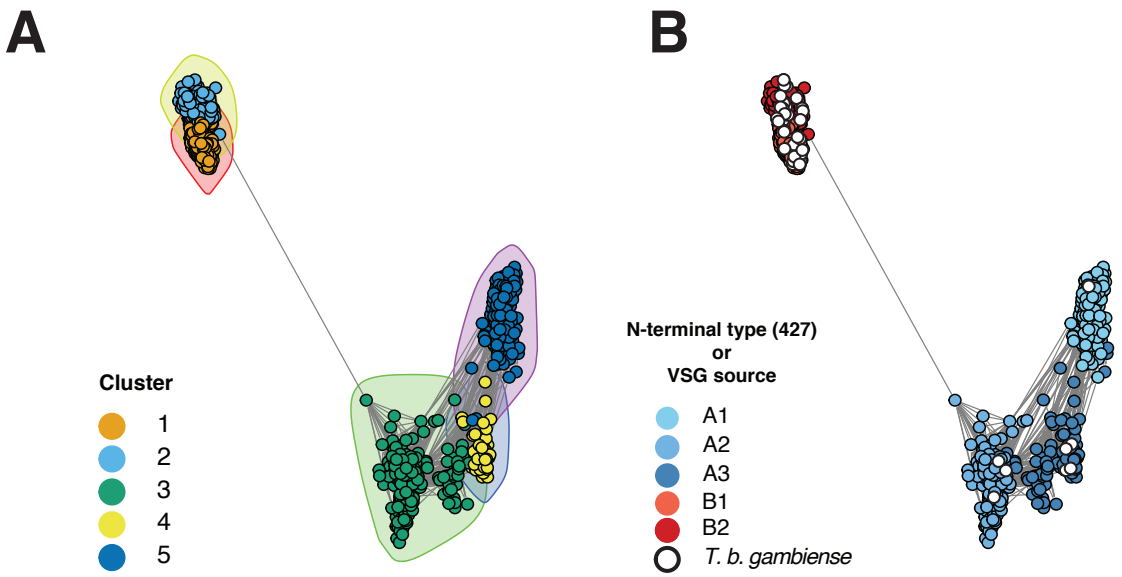

Supplemental Figure 3. (A) Network plot showing peptide sequence relatedness between N-terminal domains. Each point represents a VSG N-terminus. A link was drawn between points if BLASTp e-value was less than 10^{-2}. Colors and shaded circles represent community assignment determined by the clustering algorithm. (B) Same graph as in (A), but points are manually colored by known N-terminal subtype from Cross et al., or by subspecies for VSGs identified in patients.

821

822 **Supplemental Fig 4. BLASTp-tree of all *T. b. gambiense VSGs.*** File attached.

823

824

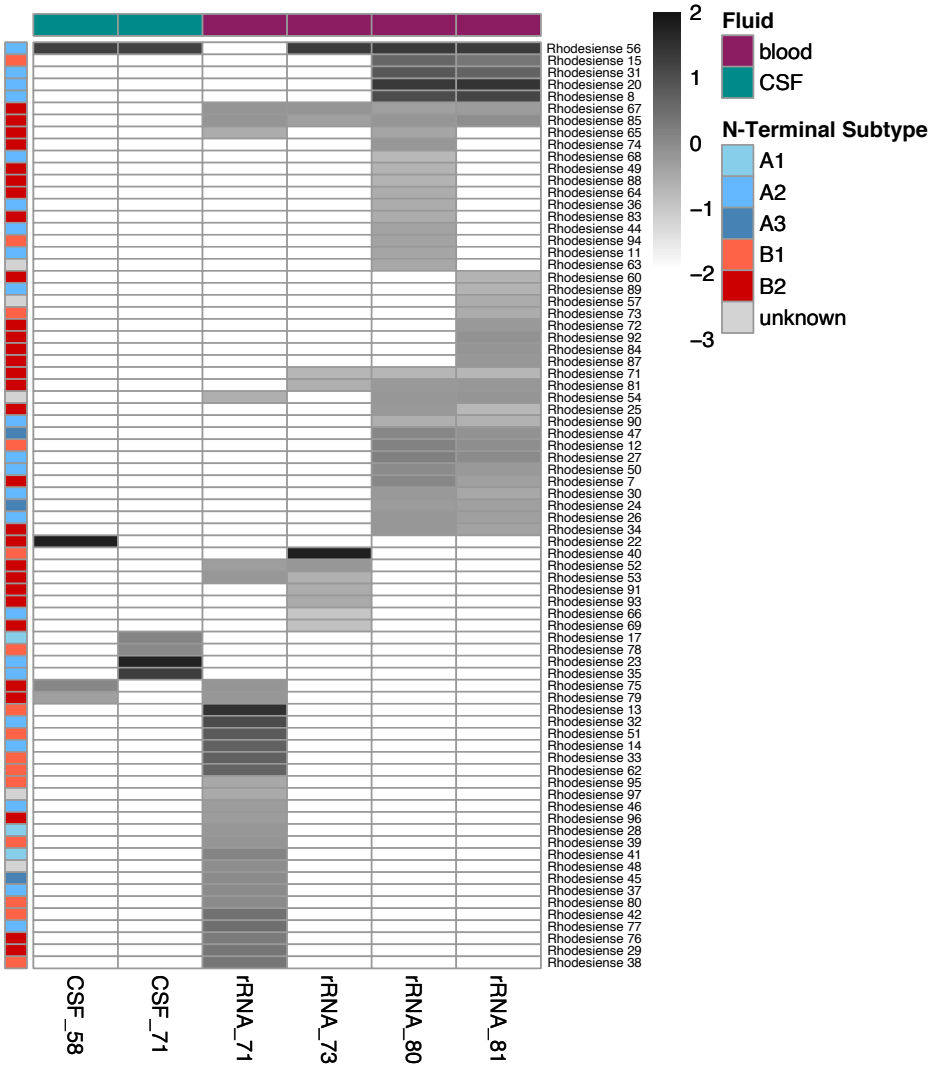

825
826 **Supplemental Figure 5. Heatmap of all assembled *T.b. rhodesiense* patient VSGs**
827
828
829
830

References

1. Romero-Meza G, Mugnier MR. Trypanosoma brucei. Trends in Parasitology. 2019. doi:10.1016/j.pt.2019.10.007
2. Büscher P, Cecchi G, Jamonneau V, Priotto G. Human African trypanosomiasis. www.thelancet.com. 2017;390. doi:10.1016/S0140-6736(17)31510-6
3. Franco JR, Cecchi G, Priotto G, Paone M, Diarra A, Grout L, et al. Monitoring the elimination of human African trypanosomiasis at continental and country level: Update to 2018. PLoS Negl Trop Dis. 2020;14: e0008261. doi:10.1371/JOURNAL.PNTD.0008261
4. Kennedy PGE, Rodgers J. Clinical and neuropathogenetic aspects of human African trypanosomiasis. Frontiers in Immunology. Frontiers Media S.A.; 2019. doi:10.3389/fimmu.2019.00039
5. Franco JR, Cecchi G, Priotto G, Paone M, Diarra A, Grout L, et al. Monitoring the elimination of human African trypanosomiasis at continental and country level: Update to 2018. PLoS Negl Trop Dis. 2020;14: e0008261. doi:10.1371/JOURNAL.PNTD.0008261
6. WHO. The Global Health Observatory. In: WHO [Internet]. World Health Organization; [cited 17 Aug 2021]. Available: https://www.who.int/data/gho/data/themes/topics/indicator-groups/indicator-group-details/GHO/human-african-trypanosomiasis
7. WHO. Ending the neglect to attain the sustainable development goals: a road map for neglected tropical diseases 2021–2030. Geneva; 2020.
8. Magez S, Caljon G, Tran T, Stijlemans B, Radwanska M. Current status of vaccination against African trypanosomiasis. Parasitology. 2010;137: 2017–2027.
9. Trindade S, Rijo-Ferreira F, Carvalho T, Pinto-Neves D, Guegan F, Aresta-Branco F, et al. Trypanosoma brucei Parasites Occupy and Functionally Adapt to the Adipose Tissue in Mice. Cell Host Microbe. 2016;19: 837–848. doi:10.1016/j.chom.2016.05.002
10. Pereira SS, Trindade S, De Niz M, Figueiredo LM. Tissue tropism in parasitic diseases. Open Biology. Royal Society Publishing; 2019. doi:10.1098/rsob.190036
11. Camara M, Soumah AM, Ilboudo H, Travaillé C, Clucas C, Cooper A, et al. Extravascular Dermal Trypanosomes in Suspected and Confirmed Cases of gambiense Human African Trypanosomiasis. Clin Infect Dis. 2021;73: 12–20. doi:10.1093/cid/ciaa897
12. Alfituri OA, Bradford BM, Paxton E, Morrison LJ, Mabbott NA. Influence of the Draining Lymph Nodes and Organized Lymphoid Tissue Microarchitecture on Susceptibility to Intradermal Trypanosoma brucei Infection. Front Immunol. 2020;11. doi:10.3389/fimmu.2020.01118
13. Marcello L, Barry JD. Analysis of the VSG gene silent archive in Trypanosoma brucei reveals that mosaic gene expression is prominent in antigenic variation and is favored by archive substructure. Genome Res. 2007;17: 1344–1352.
14. Berriman M, Ghedin E, Hertz-Fowler C, Blandin G, Renauld H, Bartholomeu DC, et al. The genome of the African trypanosome Trypanosoma brucei. Sci (New York, NY). 2005;309: 416–422.
15. Cross GAM, Kim H-S, Wickstead B. Capturing the variant surface glycoprotein

repertoire (the VSGnome) of Trypanosoma brucei Lister 427. Mol Biochem Parasitol. 2014;195: 59–73. doi:10.1016/j.molbiopara.2014.06.004

16. Müller LSM, Cosentino RO, Förstner KU, Guizetti J, Wedel C, Kaplan N, et al. Genome organization and DNA accessibility control antigenic variation in trypanosomes. Nature. 2018;563: 121–125.
17. Hall JPJ, Wang H, Barry JD. Mosaic VSGs and the scale of Trypanosoma brucei antigenic variation. Horn D, editor. PLoS Pathog. 2013;9: e1003502.
18. Jayaraman S, Harris C, Paxton E, Donachie A-M, Vaikkinen H, McCulloch R, et al. Application of long read sequencing to determine expressed antigen diversity in Trypanosoma brucei infections. Acosta-Serrano A, editor. PLoS Negl Trop Dis. 2019;13: e0007262. doi:10.1371/journal.pntd.0007262
19. Carrington M, Miller N, Blum M, Roditi I, Wiley D, Turner M. Variant specific glycoprotein of Trypanosoma brucei consists of two domains each having an independently conserved pattern of cysteine residues. J Mol Biol. 1991;221: 823–835.
20. Hutchinson OC, Smith W, Jones NG, Chattopadhyay A, Welburn SC, Carrington M. VSG structure: similar N-terminal domains can form functional VSGs with different types of C-terminal domain. Mol Biochem Parasitol. 2003;130: 127–131.
21. Jones NG, Nietlispach D, Sharma R, Burke DF, Eyres I, Mues M, et al. Structure of a glycosylphosphatidylinositol-anchored domain from a trypanosome variant surface glycoprotein. J Biol Chem. 2008;283: 3584–3593.
22. Schwede A, Jones N, Engstler M, Carrington M. The VSG C-terminal domain is inaccessible to antibodies on live trypanosomes. Mol Biochem Parasitol. 2011;175: 201–204.
23. Van Meirvenne N, Magnus E, Büscher P. Evaluation of variant specific trypanolysis tests for serodiagnosis of human infections with Trypanosoma brucei gambiense. Acta Trop. 1995;60: 189–199. doi:10.1016/0001-706X(95)00127-Z
24. A card-agglutination test with stained trypanosomes (C. A. T.T.) for the serological diagnosis of T. b. gambiense tripanosomiasis. [cited 8 Sep 2021]. Available: https://www.cabdirect.org/cabdirect/abstract/19792901755
25. Dukes P, Gibson WC, Gashumba JK, Hudson KM, Bromidge TJ, Kaukus A, et al. Absence of the LiTat 1.3 (CATT antigen) gene in Trypanosoma brucei gambiense stocks from Cameroon. Acta Trop. 1992.
26. Enyaru JCK, Allingham R, Bromidge T, Kanmogne GD, Carasco JF. The isolation and genetic heterogeneity of Trypanosoma brucei gambiense from north-west Uganda. Acta Trop. 1993.
27. Bisser S, Lumbala C, Nguertoum E, Kande V, Flevaud L, Vatunga G, et al. Sensitivity and Specificity of a Prototype Rapid Diagnostic Test for the Detection of Trypanosoma brucei gambiense Infection: A Multi-centric Prospective Study. Acosta-Serrano A, editor. PLoS Negl Trop Dis. 2016;10: e0004608. doi:10.1371/journal.pntd.0004608
28. Büscher P, Mertens P, Leclipteux T, Gilleman Q, Jacquet D, Mumba-Ngoyi D, et al. Sensitivity and specificity of HAT Sero-K-SeT, a rapid diagnostic test for serodiagnosis of sleeping sickness caused by Trypanosoma brucei gambiense: A case-control study. Lancet Glob Heal. 2014;2: e359–e363. doi:10.1016/S2214-109X(14)70203-7

29. Lumbala C, Biéler S, Kayembe S, Makabuza J, Ongarello S, Ndung'u JM. Prospective evaluation of a rapid diagnostic test for Trypanosoma brucei gambiense infection developed using recombinant antigens. PLoS Negl Trop Dis. 2018;12: e0006386. doi:10.1371/JOURNAL.PNTD.0006386
30. Mugnier MR, Cross GAM, Papavasiliou FN. The in vivo dynamics of antigenic variation in Trypanosoma brucei. Science (80-). 2015;347: 1470–1473. doi:10.1126/science.aaa4502
31. Morrison LJ, Majiwa P, Read AF, Barry JD. Probabilistic order in antigenic variation of Trypanosoma brucei. Int J Parasitol. 2005;35: 961–972.
32. Lythgoe KA, Morrison LJ, Read AF, Barry JD. Parasite-intrinsic factors can explain ordered progression of trypanosome antigenic variation. Proc Natl Acad Sci U S A. 2007;104: 8095–8100.
33. Silva Pereira S, Heap J, Jones AR, Jackson AP. VAPPER: High-throughput variant antigen profiling in African trypanosomes of livestock. Gigascience. 2019;8. doi:10.1093/gigascience/giz091
34. Pereira SS, Casas-Sánchez A, Haines LR, Ogugo M, Absolomon K, Sanders M, et al. Variant antigen repertoires in Trypanosoma congolense populations and experimental infections can be profiled from deep sequence data using universal protein motifs. Genome Res. 2018;28: 1383–1394. doi:10.1101/gr.234146.118
35. Silva Pereira S, de Almeida Castilho Neto KJG, Duffy CW, Richards P, Noyes H, Ogugo M, et al. Variant antigen diversity in Trypanosoma vivax is not driven by recombination. Nat Commun. 2020;11: 844. doi:10.1038/s41467-020-14575-8
36. Hutchinson OC, Picozzi K, Jones NG, Mott H, Sharma R, Welburn SC, et al. Variant Surface Glycoprotein gene repertoires in Trypanosoma brucei have diverged to become strain-specific. BMC Genomics. 2007;8: 234. doi:10.1186/1471-2164-8-234
37. Ilboudo H, Noyes H, Mulindwa J, Kimuda MP, Koffi M, Kaboré JW, et al. Introducing the TrypanoGEN biobank: A valuable resource for the elimination of human African trypanosomiasis. PLoS Negl Trop Dis. 2017;11: e0005438. doi:10.1371/JOURNAL.PNTD.0005438
38. Camara M, Camara O, Ilboudo H, Sakande H, Kaboré J, N'Dri L, et al. Sleeping sickness diagnosis: use of buffy coats improves the sensitivity of the mini anion exchange centrifugation test. Trop Med Int Heal. 2010;15: 796–799. doi:10.1111/J.1365-3156.2010.02546.X
39. Simarro PP, Cecchi G, Paone M, Franco JR, Diarra A, Ruiz JA, et al. The Atlas of human African trypanosomiasis: A contribution to global mapping of neglected tropical diseases. Int J Health Geogr. 2010;9: 57. doi:10.1186/1476-072X-9-57
40. González-Andrade P, Camara M, Ilboudo H, Bucheton B, Jamonneau V, Deborggraeve S. Diagnosis of trypanosomatid infections: Targeting the spliced leader RNA. J Mol Diagnostics. 2014. doi:10.1016/j.jmoldx.2014.02.006
41. Brakenhoff RH, Schoenmakers JG, Lubsen NH. Chimeric cDNA clones: a novel PCR artifact. Nucleic Acids Res. 1991;19: 1949. doi:10.1093/NAR/19.8.1949
42. Meyerhans A, Vartanian J-P, Wain-Hobson S. DNA recombination during PCR. Nucleic Acids Res. 1990;18: 1687–1691. doi:10.1093/NAR/18.7.1687
43. Grabherr MG, Haas BJ, Yassour M, Levin JZ, Thompson DA, Amit I, et al. Full-length transcriptome assembly from RNA-Seq data without a reference genome.

Nat Biotechnol. 2011;29: 644–652.

44. Li W, Godzik A. Cd-hit: a fast program for clustering and comparing large sets of protein or nucleotide sequences. Bioinformatics. 2006;22: 1658–1659.
45. Langmead B, Trapnell C, Pop M, Salzberg SL. Ultrafast and memory-efficient alignment of short DNA sequences to the human genome. Genome Biol. 2009;10: R25.
46. Storvall H, Ramsköld D, Sandberg R. Efficient and comprehensive representation of uniqueness for next-generation sequencing by minimum unique length analyses. PLoS One. 2013;8: e53822.
47. Wickstead B, Gull K. Dyneins across eukaryotes: a comparative genomic analysis. Traffic. 2007;8: 1708–1721.
48. Howe K, Bateman A, Durbin R. QuickTree: Building huge neighbour-joining trees of protein sequences. Bioinformatics. 2002;18: 1546–1547. doi:10.1093/bioinformatics/18.11.1546
49. Paradis E, Schliep K. Ape 5.0: An environment for modern phylogenetics and evolutionary analyses in R. Bioinformatics. 2019;35: 526–528. doi:10.1093/bioinformatics/bty633
50. Sievers F, Wilm A, Dineen D, Gibson TJ, Karplus K, Li W, et al. Fast, scalable generation of high-quality protein multiple sequence alignments using Clustal Omega. Mol Syst Biol. 2011;7: 539–539. doi:10.1038/msb.2011.75
51. Eddy SR. Accelerated Profile HMM Searches. PLOS Comput Biol. 2011;7: e1002195. doi:10.1371/JOURNAL.PCBI.1002195
52. Csárdi G, Nepusz T. The igraph software package for complex network research.
53. Newman MEJ. Finding community structure in networks using the eigenvectors of matrices. Phys Rev E. 2006;74: 036104. doi:10.1103/PhysRevE.74.036104
54. González-Andrade P, Camara M, Ilboudo H, Bucheton B, Jamonneau V, Deborggraeve S. Diagnosis of trypanosomatid infections: targeting the spliced leader RNA. J Mol Diagn. 2014;16: 400–404.
55. Berberof M, Pérez-Morga D, Pays E. A receptor-like flagellar pocket glycoprotein specific to Trypanosoma brucei gambiense. Mol Biochem Parasitol. 2001;113: 127–138.
56. Weirather JL, Wilson ME, Donelson JE. Mapping of VSG similarities in Trypanosoma brucei. Mol Biochem Parasitol. 2012;181: 141–152.
57. Mulindwa J, Leiss K, Ibberson D, Kamanyi Marucha K, Helbig C, Melo do Nascimento L, et al. Transcriptomes of Trypanosoma brucei rhodesiense from sleeping sickness patients, rodents and culture: Effects of strain, growth conditions and RNA preparation methods. Salavati R, editor. PLoS Negl Trop Dis. 2018;12: e0006280.
58. De Greef C, Hamers R. The serum resistance-associated (SRA) gene of Trypanosoma brucei rhodesiense encodes a variant surface glycoprotein-like protein. Mol Biochem Parasitol. 1994;68: 277–284.
59. Sistrom M, Evans B, Benoit J, Balmer O, Aksoy S, Caccone A. De Novo Genome Assembly Shows Genome Wide Similarity between Trypanosoma brucei brucei and Trypanosoma brucei rhodesiense. Louis EJ, editor. PLoS One. 2016;11: e0147660. doi:10.1371/journal.pone.0147660
60. Mugnier MR, Stebbins CE, Papavasiliou FN. Masters of Disguise: Antigenic

Variation and the VSG Coat in Trypanosoma brucei. Knoll LJ, editor. PLOS Pathog. 2016;12: e1005784. doi:10.1371/journal.ppat.1005784

61. Aitcheson N, Talbot S, Shapiro J, Hughes K, Adkin C, Butt T, et al. VSG switching in Trypanosoma brucei: antigenic variation analysed using RNAi in the absence of immune selection. Mol Microbiol. 2006;57: 1608–1622. doi:10.1111/j.1365-2958.2005.04795.x.VSG
62. Liu D, Albergante L, Newman TJ, Horn D. Faster growth with shorter antigens can explain a VSG hierarchy during African trypanosome infections: a feint attack by parasites. Sci Rep. 2018;8: 10922. doi:10.1038/s41598-018-29296-8
63. Chappuis F, Loutan L, Simarro P, Lejon V, Büscher P. Options for field diagnosis of human african trypanosomiasis. Clin Microbiol Rev. 2005;18: 133–146.
64. Truc P, Lejon V, Magnus E, Jamonneau V, Nangouma A, Verloo D, et al. Evaluation of the micro-CATT, CATT/Trypanosoma brucei gambiense, and LATEX/T b gambiense methods for serodiagnosis and surveillance of human African trypanosomiasis in West and Central Africa. Bull World Health Organ. 2002;80: 882–886.
65. Tonkin-Hill G, Ruybal-Pesántez S, Tiedje KE, Rougeron V, Duffy MF, Zakeri S, et al. Evolutionary analyses of the major variant surface antigen-encoding genes reveal population structure of Plasmodium falciparum within and between continents. PLOS Genet. 2021;17: e1009269. doi:10.1371/JOURNAL.PGEN.1009269
66. Jackson AP, Sanders M, Berry A, McQuillan J, Aslett MA, Quail MA, et al. The genome sequence of Trypanosoma brucei gambiense, causative agent of chronic human African Trypanosomiasis. PLoS Negl Trop Dis. 2010;4. doi:10.1371/journal.pntd.0000658
67. Sistrom M, Evans B, Bjornson R, Gibson W, Balmer O, Maser P, et al. Comparative genomics reveals multiple genetic backgrounds of human pathogenicity in the trypanosoma brucei complex. Genome Biol Evol. 2014;6: 2811–2819. doi:10.1093/gbe/evu222
68. Kirchgatter K, del Portillo HA. Association of Severe Noncerebral Plasmodium falciparum Malaria in Brazil With Expressed PfEMP1 DBL1α Sequences Lacking Cysteine Residues. Mol Med 2002 81. 2002;8: 16–23. doi:10.1007/BF03401999
69. Bull PC, Berriman M, Kyes S, Quail MA, Hall N, Kortok MM, et al. Plasmodium falciparum Variant Surface Antigen Expression Patterns during Malaria. PLOS Pathog. 2005;1: e26. doi:10.1371/JOURNAL.PPAT.0010026
70. Abdi AI, Hodgson SH, Muthui MK, Kivisi CA, Kamuyu G, Kimani D, et al. Plasmodium falciparum malaria parasite var gene expression is modified by host antibodies: longitudinal evidence from controlled infections of Kenyan adults with varying natural exposure. BMC Infect Dis 2017 171. 2017;17: 1–11. doi:10.1186/S12879-017-2686-0
71. Kyriacou HM, Stone GN, Challis RJ, Raza A, Lyke KE, Thera MA, et al. Differential var gene transcription in Plasmodium falciparum isolates from patients with cerebral malaria compared to hyperparasitaemia. Mol Biochem Parasitol. 2006;150: 211–218. doi:10.1016/J.MOLBIOPARA.2006.08.005
72. Duffy F, Bernabeu M, Babar PH, Kessler A, Wang CW, Vaz M, et al. Meta-analysis of plasmodium falciparum var signatures contributing to severe Malaria in

African children and Indian adults. MBio. 2019;10. doi:10.1128/MBIO.00217-19

73. Pereira SS, Casas-Sánchez A, Haines LR, Ogugo M, Absolomon K, Sanders M, et al. Variant antigen repertoires in Trypanosoma congolense populations and experimental infections can be profiled from deep sequence data using universal protein motifs. Genome Res. 2018;28: 1383. doi:10.1101/GR.234146.118

74. Silva Pereira S, Jackson AP, Figueiredo LM. Evolution of the variant surface glycoprotein family in African trypanosomes. Trends Parasitol. 2021. doi:10.1016/J.PT.2021.07.012

75. Pinger J, Nešić D, Ali L, Aresta-Branco F, Lilic M, Chowdhury S, et al. African trypanosomes evade immune clearance by O-glycosylation of the VSG surface coat. Nat Microbiol. 2018;19: 53.